# Spin-exchange cross section for a $^3He^+$ ion incident on a Rb atom

Y. Arimoto*
*Research Center for Nuclear Physics, Osaka University, Mihogaoka 10-1, Ibaraki, Osaka 567-0024, Japan*

N. Shimakura
*Department of Chemistry, Niigata University, Ikarashi, Nino-cho 8050, Niigata 950-2181, Japan*

T. Yamagata and K. Yonehara†
*Department of Physics, Konan University, Okamoto 8-9-1, Higashinada 658-8501, Kobe, Japan*

M. Tanaka
*Kobe Tokiwa College, Ohtani-cho 2-6-2, Nagata, Kobe 653-0838, Japan*

(Received 9 February 2001; revised manuscript received 12 July 2001; published 19 November 2001)

Spin-exchange cross sections between a $^3He^+$ ion and a Rb atom were calculated in a $^3He^+$ impact-energy range from 0.01 to 10 keV/amu by the semiclassical close-coupling method based on the molecular-orbital expansion. The previous calculation in which only two states of the $^3He^+$ $(1s\ ^2S)+Rb(5s\ ^2S)$ system were taken into account overestimated the experimental result at 6.33 keV/amu by orders of magnitudes, whereas the present calculation, which allowed the target excitation and electron transfer, showed a rough agreement with the experimental result. In view of the application, the spin-exchange cross sections larger than $10^{-14}$ $cm^2$, predicted at $^3He^+$ impact energies lower than 0.3 keV/amu will hopefully provide a powerful tool for producing a highly polarized $^3He$ ion beam.

DOI: 10.1103/PhysRevA.64.062714 PACS number(s): 34.50.−s, 34.10.+x

## I. INTRODUCTION

Importance of the spin-exchange processes in atomic collisions was first pointed out by Purcell and Field [1] and Wittke and Dicke [2] on the hydrogen system: They discussed the spin-exchange processes in establishing the state populations for the hyperfine levels and resulting consequences with respect to the 21-cm radio astronomy. Further, Wittke and Dicke studied the processes to experimentally redetermine the hyperfine-splitting frequency of the hydrogen atom with a high accuracy. Since their pioneering experimental work, the spin-exchange processes have been widely studied [3–7] for both fundamental research and application to such as a cryogenic hydrogen maser [8].

In recent years, production of a nuclearly polarized hydrogen or noble gas like $^3He$ received much interest due to a growing demand for application to various fields. Since the spin-exchange processes between a hydrogen/$^3He$ gas and alkali-metal atom were considered to be one of the attractive methods of polarization, their polarization mechanisms were extensively investigated [9–11].

Along with the effort to produce polarized atoms as mentioned above, much work has been done on production of polarized ions like a proton, with capture of a polarized electron by an ion (a few keV/amu) penetrating an optically pumped polarized atomic target [12–14]. The polarized-ion source based on this method called an OPPIS (optical-pumping polarized-ion source) has shown significant progress in practical use in nuclear and particle physics. Feasibility of the polarized-ion source based on the spin-exchange processes between a hydrogen and alkali-metal atom received attention as an alternative method of the OPPIS [15–18]. However, the cross sections for the spin-exchange processes between a hydrogen and alkali-metal atom was not so large that they might be used for efficiently producing a polarized proton beam.

On the other hand, the spin-exchange processes between a $^3He$ ion and alkali-metal atom had not received attention with propriety until quite recent years [19]. Recently, Arimoto *et al.* discussed the spin-exchange cross sections for the $^3He^+$-Rb system [20] to examine the validity of the EPPIS (electron-pumping polarized ion source) [21,22]. It was a great surprise that the observed upper limit for the spin-exchange cross section was almost two orders of magnitude smaller than the theoretical prediction. This unexpected result was in marked contrast with that for the H-Rb system, where the theory satisfactorily reproduced the experimental results [15–18]. The above aspects suggest the complexity of the spin-exchange processes for the $^3He^+$-Rb system. In fact, this complexity may come from the following expectation: The singlet states of the H+Rb system are subject to strong ionic covalent interaction, which leads to a deep potential well at fairly short internuclear distances, whereas the triplet states are not. Also, the energy of the initial state for the $He^+ + Rb$ system is accidentally close to the energy of the states populated by the charge transfers. As a result, translation effects tend to be more important in the $He^+ + Rb$ system than in the H+Rb system.

Thus, a primary concern of the present work is to disen-

*Present address: Japan Synchrotron Radiation Research Institute (JASRI), Kouto 1-1-1, Mikazuki-cho, Sayo, Hyogo 679-5198, Japan.

†Present address: Physics Department, University of Michigan, Ann Arbor, Michigan 48109.

 

TABLE I. Orbital exponents of the Slater-type basis.

| He | | | Rb | |
|---|---|---|---|---|
| $1s$ | 2.9110000 | | $4s$ | 1.47256 |
| | 2.0000000 | | $5s$ | 1.45575 |
| | 1.4530000 | | | 0.83134 |
| | 1.0000000 | | | 0.45312 |
| $2s$ | 1.3093953 | (1.4530000) | $5p$ | 1.06297 |
| | 0.5372721 | (1.0000000) | | 0.67145 |
| $2p$ | 0.7167531 | (1.6998674) | | |
| | 0.5057654 | (0.5314231) | | |

[a]Values in parentheses correspond to the triplet manifold.

tangle the problem associated with the spin-exchange cross sections for the $^3He^+$-Rb system in a quantitative way. We performed the calculation of the spin-exchange cross sections by the semiclassical close-coupling method based on the molecular-orbital expansion not only for two states of the $^3He^+$ $(1s\ ^2S)+Rb(5s\ ^2S)$ system but also for the states populated via the target excitation and the charge transfer.

## II. THEORETICAL APPROACH

In this section, we present a summary of the calculation of the spin-exchange cross sections for the $^3He^+$-Rb system. An evolution of the formalism describing the spin-exchange cross sections is outlined in the Appendix.

Since the details of the present theoretical method, i.e., the semiclassical close-coupling method based on the molecular-orbital expansion were described previously [23,24], only a brief summary of the basic technique and specific information used for the present calculation are given here.

We assume that the initial state is $He^+(1s)+Rb(5s)$ for a large internuclear distance, whereas, at a finite internuclear distance this state becomes a singlet and triplet molecular state denoted by $1\ ^1\Sigma$ and $1\ ^3\Sigma$. We carry out the semiclassical close-coupling calculations based on the molecular-orbital expansion; the internal electron motions are treated quantum mechanically, while the relative motions of nuclei are treated as the straight-line trajectories classically. A plane-wave-type electron-translation factor (ETF) is employed in the first order of the relative velocity.

The above model is valid for low impact energies higher than 20 eV/amu. It is still controversial whether or not our model is valid at impact energies higher than 1 keV/amu. However, since there are reports that discuss validity of the model up to $\sim$10 keV/amu [25,26], we consider that our method could be effective up to this energy region.

TABLE II. $Rb^+$ pseudopotential.

| | |
|---|---|
| $A_0$ | 17.29503 |
| $A_1$ | 2.851747 |
| $A_2$ | $-1.553162$ |
| $\xi_0$ | 0.746748 |
| $\xi_1$ | 0.295391 |
| $\xi_2$ | 0.387761 |
| $d$ | 1.950 |
| $\alpha_d$ | 8.966 |
| $\alpha_q$ | 102.0 |

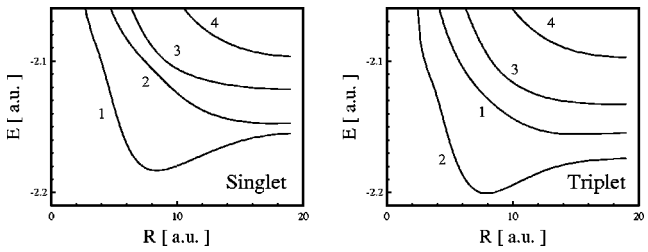


FIG. 1. Potential-energy curves for the singlet (left curves) and triplet (right curves) $(He\text{-}Rb)^+$ quasimolecule states. The numbers indicated are referred to in the text.

### A. Electronic states

The adiabatic potential energies for $(He\text{-}Rb)^+$ are obtained by the valence-band configuration-interaction method modified by inclusion of a pseudopotential to describe the atomic core of $Rb^+$. The pseudopotential used is a Gaussian-type one [27], viz.,

$$V(\vec{r})=\sum_l V_l(r)|Y_{lm}\rangle\langle Y_{lm}|, \tag{1}$$

where $Y_{lm}$ are a spherical harmonics and $V_l(r)$ is given by

$$V_l(\vec{r})=A_l e^{-\xi_l r^2}-\frac{\alpha_d}{2(r^2+d^2)^2}-\frac{\alpha_q}{2(r^2+d^2)^3}-\frac{1}{r}. \tag{2}$$

The values of the pseudopotential parameters are referred to the review given by Bardsley [27] and also to the previous work by Stevens *et al.* [28]. In Ref. [27] the Rb pseudopotentials include $l=3$ terms, but these were not used in the present calculation. The orbital exponents of the Slater-type orbital for the valence electron of Rb atom were taken from the previous work by Stevens *et al.* [28], while those for the $He^+$ ion and He atom were obtained by variationally optimizing the energies. The Slater exponents and the pseudopotential parameters are given in Tables I and II, respectively.

The potential-energy curves for the $(He\text{-}Rb)^+$ quasimolecule states calculated by the above method are shown in Fig. 1 as a function of the internuclear separation between the $^3He$ nucleus and Rb core. The left curves in Fig. 1 show the energy curves for the singlet states and the right ones show those for triplet states. The numbers in these figures are referred to in Sec. II B. In order to examine the precision of the calculated results, we estimated the ionization potentials for Rb and $^3He$. It was found that the deviation of the calculated results from the spectroscopic data [29,30] was smaller than 0.062 eV.

### B. Collision dynamics

The total scattering wave function was expanded in terms of products of the molecular electronic states and atomic-

type ETF's. Substituting the total wave function into the time-dependent Schrödinger equation and retaining the ETF correction up to the first order in the relative velocity yielded a set of first-order coupled differential equations. By numerically solving the coupled equations, we obtain the scattering amplitudes for transitions. The squared amplitude gives the transition probability, and the probability times the impact parameter integrated over the impact parameter gives the cross section.

In the dynamical calculations, the following eight $\Sigma$ states were taken into account:

| State | Symmetry | Asymptotic limit |
|---|---|---|
| 1 | $^{1,3}\Sigma$ | $\rightarrow {}^3He^+(1s\ ^2S)+Rb(5s\ ^2S)$ |
| 2 | $^{1,3}\Sigma$ | $\rightarrow {}^3He(1s2s\ ^{1,3}S)+Rb^+$ |
| 3 | $^{1,3}\Sigma$ | $\rightarrow {}^3He(1s2p\ ^{1,3}P)+Rb^+$ |
| 4 | $^{1,3}\Sigma$ | $\rightarrow {}^3He^+(1s\ ^2S)+Rb(5p\ ^2P)$ |

The initial wave function $\Psi_I$ is a linear superposition of the $1\ ^1\Sigma$ and $1\ ^3\Sigma$ wave functions at a separated atom limit as given in Eq. (A8) in the Appendix [10,15]. As a collision pair approach each other, both of the $1\ ^1\Sigma$ and $1\ ^3\Sigma$ states couple with the singlet and triplet excitation/charge-transfer channels, respectively. The wave function during the collision is expressed as a function of time by

$$\Psi_I(t)=\sum_{\lambda=1}^{4} c_\lambda(t)\Phi_{\lambda^1\Sigma}F_\lambda+\sum_{\lambda=1}^{4} c'_\lambda(t)\Phi_{\lambda^3\Sigma}F'_\lambda, \qquad (3)$$

where $\lambda$ is the state number for the $(He\text{-}Rb)^+$ molecule, $\Phi_{\lambda^1\Sigma}$ ($\Phi_{\lambda^3\Sigma}$) and $F_\lambda$ ($F'_\lambda$) are the electronic wave function and ETF for the state of $\lambda^1\Sigma$ ($\lambda^3\Sigma$), respectively. The above coefficient, $c_\lambda(t)$ or $c'_\lambda(t)$ is normalized as follows:

$$\sum_{\lambda=1}^{4} c_\lambda(t)^2=\sum_{\lambda=1}^{4} c'_\lambda(t)^2=\frac{1}{2}. \qquad (4)$$

The radial-coupling matrix elements necessary for solving the coupled equations are numerically evaluated according to the prescription given by Kimura and Lane [23]. The calculated results are shown in Fig. 2 for the singlet [(a)–(d)] and for the triplet states [(e)–(h)], respectively, where the numbers in the insets of Fig. 2 indicate the state numbers of the $(He\text{-}Rb)^+$ system.

The initial condition must satisfy the following relations at $t=-\infty$:

$$c_1(-\infty)=c'_1(-\infty)=\frac{1}{\sqrt{2}}, \qquad (5)$$

$$c_\lambda(-\infty)=c'_\lambda(-\infty)=0 \quad (\lambda\neq 1). \qquad (6)$$

After the collision, the probability that the spin exchange has occurred is given by the superposition of the survived amplitude for the $1\ ^1\Sigma$ and $1\ ^3\Sigma$ states according to the prescription described in the Appendix as

$$P(\mathrm{I}\rightarrow\mathrm{II})=\frac{1}{2}\left|-c_1(t)+c'_1(t)\exp\left\{-\frac{i}{\hbar}\int_{-\infty}^{t}(V_t-V_s)dt\right\}\right|^2, \qquad (7)$$

where $V_s(V_t)$ is the potential energy of the $1\ ^1\Sigma$ ($1\ ^3\Sigma$) state, respectively. The spin-exchange cross section is given by

$$\sigma_{se}=2\pi\int_0^\infty \frac{b}{2}\left|-c_1(\infty)+c'_1(\infty)e^{-i\phi_{ts}}\right|^2 db, \qquad (8)$$

where $\phi_{ts}$ is a phase difference defined in Eq. (A16) in the Appendix. In this calculation, we neglected the contribution of state 4 to $\sigma_{se}$ because our close-coupling results showed that the excitation probability to this state and the phase difference were very small as compared with that of state 1.

## III. RESULT AND DISCUSSION

The calculated spin-exchange cross sections are plotted in Fig. 3(a) as a function of $^3He^+$ impact energy, where a dashed curve is the result of the calculation taking only two states of the $^3He^+(1s\ ^2S)+Rb(5s\ ^2S)$ among the eight $\Sigma$ states, and closed triangles are the results of the eight-state calculation. Here, a solid curve is drawn as a guide to the eye to connect the closed triangles. An experimental result (a closed circle with an error bar) is also plotted in this figure. It is instructive to mention that the dashed curve shows an oscillatory pattern and a gentle decrease with an increase of impact energy. The oscillatory pattern is caused by a periodic exchange of electrons between a Rb atom and a $^3He^+$ ion during the collision, and the gentle decrease is caused by a decrease of $\phi_{ts}$ according to an increase of impact energy [see Eq. (A16) in the Appendix]. It is, however, emphasized again that the results deduced from the two-state calculation, in which only two states of the $^3He^+(1s\ ^2S)+Rb(5s\ ^2S)$ are taken into account, are almost two orders of magnitude larger than the experimental result at 6.33 keV.

On the other hand, the spin-exchange cross sections resulting from the eight-state calculation show behavior greatly different from that obtained by the two-state calculation; the closed triangles almost agree with the dashed curve for impact energies lower than 0.1 keV/amu, while they decrease more rapidly than the dashed curve at impact energies higher than 0.3 keV/amu. Consequently, the eight-state calculation agrees with the experimental result though the calculation still overestimates the experimental result somehow. The rapid decrease of the spin-exchange cross sections at higher energies demonstrates that the effect of the eight states becomes more significant when the impact energy is increased. In fact, from Fig. 3(b), it can be seen that both the electron capture and target-excitation cross sections increase as the energy increase, though contribution from the latter cross sections is less significant.

In the present work, we have taken only four $\Sigma$-type charge-transfer states into account for simplicity. If one takes the effects of other $\Sigma$-type charge transfers or the $\Pi$ formation, one can expect that the calculation will result in a better agreement with the experimental result. The spin-exchange cross section caused by the $5p$ state in Rb may also modify the present result. Since the exact treatment needs further elaborate work, we made a rough estimation of the spin-exchange cross section via the $5p$ state. The calculated result was found to be less than $2\times10^{-17}$ cm$^2$. From this result it

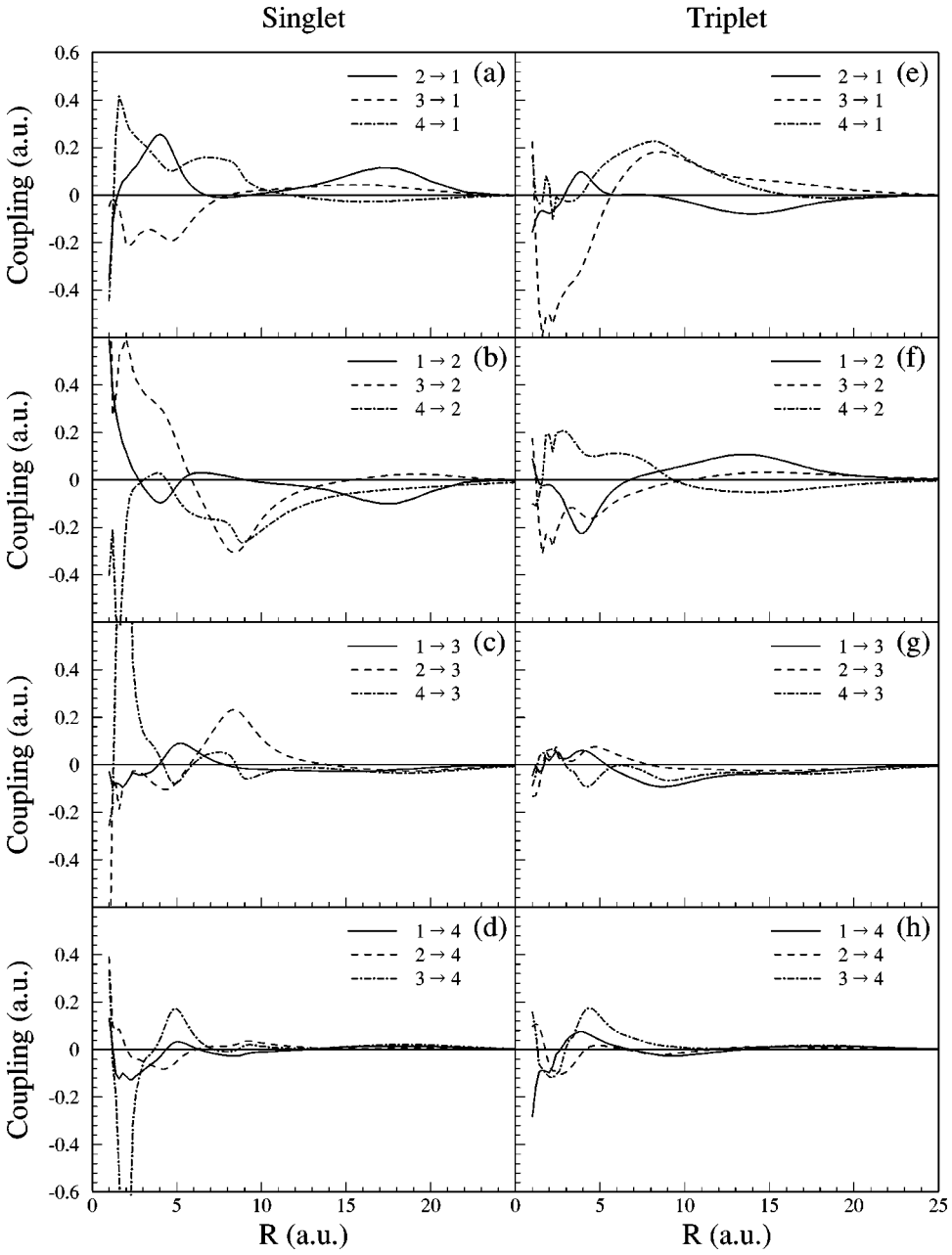


FIG. 2. The calculated results for the radial-coupling matrix elements for the singlet [(a)–(d)] and triplet [(e)–(h)] states of the $He^+$-Rb system, where the numbers in the insets indicate the state numbers of the $(He\text{-}Rb)^+$ system (see Sec. II B).

is concluded that the contribution from this state is less important in evaluating the spin-exchange cross sections by the eight-state calculation.

## IV. CONCLUSION

The starting point of the present work is to investigate the origin of discrepancy between the experimental result and the calculated one based on the two-state calculation for the spin-exchange cross section of the $^3He^+$-Rb system [20]. For this purpose, we have employed the semiclassical close-coupling method based on the molecular-orbital expansion allowing the charge transfers and target excitations. The calculation was performed in a wide $^3He^+$ impact energy covering a range from 0.01 to 10 keV/amu. The calculated results showed that the eight-state calculation did not affect the spin-exchange process at a $^3He^+$ impact energy lower than 0.3 keV, while at higher impact energy than that it becomes seriously influential. This result shows that the effect of the eight-state calculation acts on reducing the spin-exchange cross section. As a result, the experimental spin-exchange cross section was quantitatively reproduced by the present ''eight-state calculation.''

Another important aspect deduced from the present result is the possibility that the large spin-exchange cross section at low impact energy may be useful to produce a highly polarized $^3He$ nucleus. At a $^3He^+$ impact energy lower than 0.3 keV/amu, the spin-exchange cross section exceeds $10^{-14}$ $cm^2$, which is comparable to a charge-transfer cross section [31,32]. This will hopefully enable us to produce a polarized $^3He$ beam with a polarized Rb vapor with low density by means of the spin-exchange process, because a

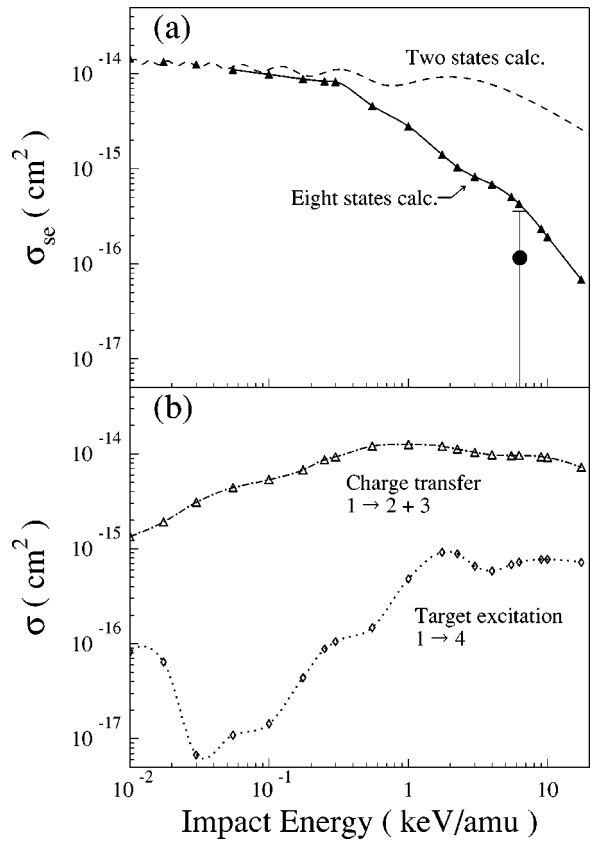


FIG. 3. (a) Calculated $\sigma_{se}$ as a function of impact energy of $^3He^+$ ion, where the dashed curve is $\sigma_{se}$ calculated with the two states, and closed triangles and solid curve are $\sigma_{se}$ calculated with eight states. (b) Calculated cross sections for the charge-transfer (open triangles and a dot-dashed curve) and target-excitation (open diamonds and a dotted curve) channels. Numbers indicated are states defined in the text.

fully polarized Rb vapor with such low density can be practically available with ease [33].

## ACKNOWLEDGMENTS

This work has been performed under the support of the Research Center for Nuclear Physics (RCNP) Cyclotron Facility at Osaka University and a Grant-in-Aid from the Ministry of Education of Japan. The authors are indebted to the RCNP director, Professor Y. Nagai for his support of the project on the polarized-$^3$He-ion source. They also wish to express their sincere appreciation to the RCNP former directors, Professor H. Ejiri and Professor M. Fujiwara (RCNP), Professor L. W. Anderson (Wisconsin), Professor R. Morgenstern (KVI), Professor A. N. Zelenski (TRIUMF), Dr. T. Takeuchi (University of Tokyo), and Professor Y. Plis (Dubna) for their encouragement throughout this work.

## APPENDIX: QUANTUM-MECHANICAL TREATMENT OF THE SPIN-EXCHANGE CROSS SECTION

In this appendix, we present a brief review of the quantum-mechanical treatment for the spin-exchange process between a $^3He^+$ ion beam and Rb atom target by modifying the prescription given by Swenson *et al.* [15] so that the relevant physics might be clear in terms of the Heisenberg expression.

Suppose that an incident and outgoing channel is described by $^3He^+(1s\ ^2S)+Rb(5s\ ^2S)$ and during the collision no target excitation or electron transfer occurs. The spin-exchange processes are induced by electron exchange between a $^3He^+$ ion and a Rb atom during the collision, and the spin-exchange process is schematically expressed by

$$^3He^+\downarrow + Rb\uparrow \rightarrow {}^3He^+\uparrow + Rb\downarrow, \tag{A1}$$

where the arrow direction indicates the spin direction (up or down) for an electron of either $^3$He ion or for the valence electron of Rb atom.

This process is treated quantum mechanically by the following scenario, where we assume that the collisions occur under the presence of the magnetic field strong enough to decouple the hyperfine couplings, where the nuclear spin effects could be ignored. The spin functions of the two colliding atomic system are represented as being a superposition of a singlet and a triplet function. Through the collision a phase shift occurs between the amplitude of the singlet component and that of the triplet one due to the difference in scattering potential of the two components, which eventually gives rise to the spin-exchange process.

Bearing this in mind, we will formulate a spin-exchange cross section. As possible molecular states, we take only the $1\Sigma$ states (singlet $^1\Sigma$ and triplet $^3\Sigma$) into account. Antisymmetrized wave functions for the singlet and triplet states of the collisional $(He\text{-}Rb)^+$ system are, respectively, given by

$$\Phi_{^1\Sigma} = \frac{1}{2}\{\alpha(1)\beta(2)-\beta(1)\alpha(2)\} \times\{\phi_{Rb}(1)\phi_{He}(2)+\phi_{He}(1)\phi_{Rb}(2)\}, \tag{A2}$$

$$\Phi_{^3\Sigma} = \frac{1}{2}\{\alpha(1)\beta(2)+\beta(1)\alpha(2)\} \times\{\phi_{Rb}(1)\phi_{He}(2)-\phi_{He}(1)\phi_{Rb}(2)\}, \tag{A3}$$

where $\alpha(\beta)$ is an electron spin-up (-down) wave function, and $\phi_{He}$ ($\phi_{Rb}$) is a spatial part of the wave function for the electron of $^3He^+$ ion (valence electron of Rb atom), respectively.

On the other hand, the wave function with $m_z=+1/2$ for a Rb atom and with $m_z=-1/2$ for a $^3He^+$ ion is written as

$$\Psi_I = \frac{1}{\sqrt{2}}\begin{vmatrix}\alpha(1)\phi_{Rb}(1) & \beta(1)\phi_{He}(1)\\ \alpha(2)\phi_{Rb}(2) & \beta(2)\phi_{He}(2)\end{vmatrix} \tag{A4}$$

$$= \frac{1}{\sqrt{2}}\{\alpha(1)\phi_{Rb}(1)\beta(2)\phi_{He}(2) - \alpha(2)\phi_{Rb}(2)\beta(1)\phi_{He}(1)\}. \tag{A5}$$

In a similar way, the wave function with $m_z=-1/2$ for a Rb atom and with $m_z=+1/2$ for a $^3He^+$ ion is written as

$$\Psi_{\mathrm{II}}=\frac{1}{\sqrt{2}}\begin{vmatrix}\beta(1)\phi_{\mathrm{Rb}}(1) & \alpha(1)\phi_{\mathrm{He}}(1)\\ \beta(2)\phi_{\mathrm{Rb}}(2) & \alpha(2)\phi_{\mathrm{He}}(2)\end{vmatrix} \tag{A6}$$

$$=\frac{1}{\sqrt{2}}\{\beta(1)\phi_{\mathrm{Rb}}(1)\alpha(2)\phi_{\mathrm{He}}(2) - \beta(2)\phi_{\mathrm{Rb}}(2)\alpha(1)\phi_{\mathrm{He}}(1)\}. \tag{A7}$$

From Eqs. (A2), (A3), (A5), and (A7), $\Psi_{\mathrm{I}}$ and $\Psi_{\mathrm{II}}$ are given as a superposition of $\Phi_{^1\Sigma}$and $\Phi_{^3\Sigma}$by using the matrix expression

$$\begin{pmatrix}\Psi_{\mathrm{I}}\\ \Psi_{\mathrm{II}}\end{pmatrix}=\begin{pmatrix}\cos\theta & \sin\theta\\ -\sin\theta & \cos\theta\end{pmatrix}\begin{pmatrix}\Phi_{^1\Sigma}\\ \Phi_{^3\Sigma}\end{pmatrix}, \tag{A8}$$

where $\theta$ is called a mixing angle, and in the present case, $\theta$ should be equal to $\pi/4$. Let $\Psi_{\mathrm{I}}(t)$ $[\Psi_{\mathrm{II}}(t)]$ be the wave function at time $t$. We assume that at time $t=-\infty$, an internuclear separation is infinite, and at time $t=0$, a $^3\mathrm{He}^+$ ion approaches closest to a Rb atom. The wave functions $\Psi_{\mathrm{I}}(t)$ and $\Psi_{\mathrm{II}}(t)$ are expressed as

$$\begin{pmatrix}\Psi_{\mathrm{I}}(t)\\ \Psi_{\mathrm{II}}(t)\end{pmatrix}=\begin{pmatrix}\cos\theta & \sin\theta\\ -\sin\theta & \cos\theta\end{pmatrix}\exp\left(-\frac{i}{\hbar}\int_{-\infty}^{t}H\,dt\right)\begin{pmatrix}\Phi_{^1\Sigma}\\ \Phi_{^3\Sigma}\end{pmatrix}, \tag{A9}$$

where $H$ is a Hamiltonian whose eigenfunctions and eigenvalues are $\Phi_{^1\Sigma}$, $\Phi_{^3\Sigma}$and $V_{\mathrm{s}}$, $V_{\mathrm{t}}$, respectively. Here, we define $E(t,V)$ as

$$E(t,V)=\exp\left(-\frac{i}{\hbar}\int_{-\infty}^{t}V\,dt\right). \tag{A10}$$

By substituting Eq. (A8) in Eq. (A9), Eq. (A9) is rewritten using the Heisenberg expression as

$$\begin{aligned}\begin{pmatrix}\Psi_{\mathrm{I}}(t)\\ \Psi_{\mathrm{II}}(t)\end{pmatrix}&=\begin{pmatrix}\cos\theta & \sin\theta\\ -\sin\theta & \cos\theta\end{pmatrix}\begin{pmatrix}E(t,V_{\mathrm{s}}) & 0\\ 0 & E(t,V_{\mathrm{t}})\end{pmatrix}\begin{pmatrix}\cos\theta & -\sin\theta\\ \sin\theta & \cos\theta\end{pmatrix}\begin{pmatrix}\Psi_{\mathrm{I}}\\ \Psi_{\mathrm{II}}\end{pmatrix}\\ &=\begin{pmatrix}E(t,V_{\mathrm{s}})\cos^2\theta+E(t,V_{\mathrm{t}})\sin^2\theta & [-E(t,V_{\mathrm{s}})+E(t,V_{\mathrm{t}})]\sin\theta\cos\theta\\ [-E(t,V_{\mathrm{s}})+E(t,V_{\mathrm{t}})]\sin\theta\cos\theta & E(t,V_{\mathrm{s}})\cos^2\theta+E(t,V_{\mathrm{t}})\sin^2\theta\end{pmatrix}\begin{pmatrix}\Psi_{\mathrm{I}}\\ \Psi_{\mathrm{II}}\end{pmatrix}\\ &=U\begin{pmatrix}\Psi_{\mathrm{I}}\\ \Psi_{\mathrm{II}}\end{pmatrix}.\end{aligned} \tag{A11}$$

The matrix $U$ is the time-evolution operator.

The probability that a state $i$ becomes a state $j$ at $t$ is given by

$$P(i\to j)=U_{ij}^{*}U_{ij} \tag{A12}$$

$$=\begin{cases}1-\sin^2 2\theta\sin^2\left[\dfrac{\phi_{\mathrm{ts}}(t)}{2}\right] & (i=j)\\ \sin^2 2\theta\sin^2\left[\dfrac{\phi_{\mathrm{ts}}(t)}{2}\right] & (i\neq j),\end{cases} \tag{A13}$$

where $\phi_{\mathrm{ts}}(t)$ is expressed by

$$\phi_{\mathrm{ts}}(t)=\int_{-\infty}^{t}(V_{\mathrm{t}}-V_{\mathrm{s}})/\hbar\,dt. \tag{A14}$$

In consequence, the spin-exchange cross section is obtained by summing up the above probability $P(\mathrm{I}\to\mathrm{II})$ at $t=+\infty$ with respect to the impact parameter $b$.

$$\sigma_{\mathrm{se}}=2\pi\int_{0}^{\infty}b\sin^2\frac{\phi_{\mathrm{ts}}}{2}db, \tag{A15}$$

where $\sin^2(2\theta)=1$ is used because of $\theta=\pi/4$. On the basis of the semiclassical impact-parameter approximation, in which the $^3\mathrm{He}^+$ trajectory is expressed by a straight line, $\phi_{\mathrm{ts}}(\infty)$ is given by

$$\phi_{\mathrm{ts}}=-2\int_{b}^{\infty}\frac{R(V_{\mathrm{t}}-V_{\mathrm{s}})}{\hbar v\sqrt{R^2-b^2}}dR, \tag{A16}$$

where $R$ is an internuclear separation of the two atoms and $v$ is the relative velocity of the two atoms.

[1] E.M. Purcell and G.B. Field, Astrophys. J. **124**, 542 (1956).
[2] J.P. Wittke and R.H. Dicke, Phys. Rev. **103**, 620 (1956).
[3] B.J. Verhaar, J.M.V.A. Koelman, H.T.C. Stoof, O.J. Luiten, and S.B. Crampton, Phys. Rev. A **35**, 3825 (1987).
[4] J.M.V.A. Koelman, S.B. Crampton, H.T.C. Stoof, O.J. Luiten, and B.J. Verhaar, Phys. Rev. A **38**, 3535 (1988).
[5] J.M.V.A. Koelman, S.B. Crampton, H.T.C. Stoof, O.J. Luiten, and B.J. Verhaar, *Spin Polarized Quantum Systems*, edited by S. Stringari (World Scientific, Singapore, 1989), p. 223.
[6] W. Jitschin, S. Osimitsch, H. Reihl, D.W. Mueller, H. Klein-

poppen, and H.O. Lutz, Phys. Rev. A **34**, 3684 (1986).
[7] S. Osimitsch, W. Jitschin, H. Reihl, H. Kleinpoppen, H.O. Lutz, O. Mó, and A. Riera, Phys. Rev. A **40**, 2958 (1989).
[8] M.E. Hayden, M.D. Hürlimann, and W.N. Hardy, Phys. Rev. A **53**, 1589 (1996).
[9] S.G. Redsun, R.J. Knize, G.D. Cates, and W. Happer, Phys. Rev. A **42**, 1293 (1990).
[10] H.R. Cole and R.E. Olson, Phys. Rev. A **31**, 2137 (1985).
[11] A. Dalgarno and M.R. Rudge, Proc. R. Soc. London, Ser. A **286**, 519 (1965).
[12] W. Haeberli, in *Proceedings of the 2nd Symposia on Polarization Phenomena in Nuclear Reactions*, edited by P. Huber and H. Schopper (Birkhauser Basel, 1965), p. 64.
[13] L.W. Anderson, Nucl. Instrum. Methods **167**, 363 (1979).
[14] Y. Mori, A. Takagi, K. Ikegami, S. Fukumoto, and A. Ueno, J. Phys. Soc. Jpn. **55**, 453 (1986).
[15] D.R. Swenson, D. Tupa, and L.W. Anderson, J. Phys. B **18**, 4433 (1985).
[16] D.R. Swenson, D. Tupa, and L.W. Anderson, Helv. Phys. Acta **59**, 662 (1986).
[17] A.N. Zelenski and S.A. Kokhanovski, in *Polarized Ion Sources and Polarized Gas Targets*, edited by L.W. Anderson and Willy Haeberli, AIP Conf. Proc. 293 (AIP, New York, 1994), p. 164.
[18] A.N. Zelenski, C.D.P. Levy, W.T.H. van Oers, P.W. Schmor, J. Welz, and G.W. Wight, in *Polarization Phenomena in Nuclear Physics*, edited by Edward J. Stephenson and Steven E. Vigdor, AIP Conf. Proc. 339 (AIP, New York, 1995), p. 650.
[19] *Proceedings of the 7th RCNP International Workshop on Polarized $^3$He Beams and Gas Targets and Their Application, Kobe, Japan, 1997*, edited by M. Tanaka (North-Holland, Amsterdam, 1998).
[20] Y. Arimoto, N. Shimakura, K. Yonehara, T. Yamagata, and M. Tanaka, Eur. Phys. J. D **8**, 305 (2000).
[21] M. Tanaka, M. Fujiwara, S. Nakayama, and L.W. Anderson, Phys. Rev. A **52**, 392 (1995).
[22] M. Tanaka, T. Yamagata, K. Yonehara, T. Takeuchi, Y. Arimoto, M. Fujiwara, Y. Plis, L.W. Anderson, and R. Morgenstern, Phys. Rev. A **60**, R3354 (1999).
[23] M. Kimura and N.F. Lane, Adv. At., Mol., Opt. Phys. **26**, 76 (1989).
[24] N. Shimakura and M. Kimura, Phys. Rev. A **44**, 1659 (1991).
[25] N. Shimakura, H. Sato, M. Kimura, and T. Watanabe, J. Phys. B **20**, 1801 (1987).
[26] A. Kumar, N.F. Lane,and M. Kimura, Phys. Rev. A **42**, 3861 (1990).
[27] J.N. Bardsley, Case Stud. At. Phys. **4**, 299 (1974).
[28] W.J. Stevens, A.M. Karo, and J.R. Hiskes, J. Chem. Phys. **74**, 3989 (1981).
[29] S. Bashkin and J. R. Stoner, *Atomic Energy Levels and Grotorian Diagrams I* (North-Holland, Amsterdam, 1975).
[30] C. E. Moor, *Atomic Energy Levels*, Natl. Bur. Stand. Ref. Data Ser., Natl. Bur. Stand. (U.S.) Circ. No. 467 (U.S. GPO, Washington, D.C., 1949), Vols. I and II.
[31] J.R. Peterson and D.C. Lorents, Phys. Rev. **182**, 152 (1969).
[32] R.J. Girnius and L.W. Anderson, Nucl. Instrum. Methods **137**, 373 (1976).
[33] K. Yonehara, T. Yamagata, T. Takeuchi, Y. Arimoto, and M. Tanaka, Nucl. Instrum Methods Phys. Res. B **184**, 391 (2001).